

Published in final edited form as:

*Sci Signal.* ; 8(372): ra35. doi:10.1126/scisignal.aaa0441.

## Casein kinase 2 (CK2) phosphorylates the deubiquitylase OTUB1 at Ser<sup>16</sup> to trigger its nuclear localization

Lina Herhaus<sup>1</sup>, Ana B. Perez-Oliva<sup>1</sup>, Giorgio Cozza<sup>2</sup>, Robert Gourlay<sup>1</sup>, Simone Weidlich<sup>1</sup>, David G. Campbell<sup>1</sup>, Lorenzo A. Pinna<sup>2</sup>, and Gopal P. Sapkota<sup>1,\*</sup>

<sup>1</sup>MRC Protein Phosphorylation Unit, College of Life Sciences, University of Dundee, Dow Street, Dundee, DD1 5EH, Scotland, United Kingdom.

<sup>2</sup>Department of Biomedical Sciences and CNR Institute of Neurosciences, University of Padova, via Ugo Bassi 58/B, 35131 Padova, Italy.

### Abstract

The deubiquitylating enzyme OTUB1 is present in all tissues and targets a multitude of substrates, both in the cytosol and nucleus. Here, we found that the phosphorylation of OTUB1 at Ser<sup>16</sup> and its subsequent nuclear accumulation is mediated by casein kinase 2 (CK2). Whereas unphosphorylated OTUB1 was detected mainly in the cytosol, Ser<sup>16</sup>-phosphorylated OTUB1 was detected only in the nucleus. Pharmacological inhibition or genetic ablation of CK2 blocked the phosphorylation of OTUB1 at Ser<sup>16</sup> and its nuclear localization in various cells. The phosphorylation of OTUB1 at Ser<sup>16</sup> did not alter its catalytic activity in vitro, its ability to bind K63-linked ubiquitin chains in vitro and its ability to interact with the E2 enzyme UBE2N in vitro. The phosphorylation at Ser<sup>16</sup> and subsequent nuclear localization of OTUB1 was essential for cells to repair ionizing radiation-induced DNA damage in osteosarcoma U2OS cells.

### Introduction

OTUB1 is a member of the ovarian tumour domain protease (OTU) family of deubiquitylating enzymes (DUBs) (1). DUBs are isopeptidases that remove attached ubiquitin chains or molecules from their targets (2). In general DUBs are known to target a multitude of substrates for deubiquitylation. Therefore, it is likely that their activity, target recognition as well as subcellular localization are tightly regulated. OTUB1 protein is detected ubiquitously in tissues and recent reports have shed light into the molecular functions of OTUB1 in deubiquitylating K48-linked ubiquitin chains as well as inhibiting the action of E2 ubiquitin-conjugating enzymes (1, 3-10). OTUB1 has been reported to

\*Corresponding author. g.sapkota@dundee.ac.uk.

**Author contributions:** LH designed, performed and analysed most of the experiments and helped with the preparation of the manuscript. AP performed experiments related to DNA damage responses and nuclear import/export of OTUB1 and analysed data. GC and LP generated TDB and performed in vitro CK2 assays on peptide substrates. RG and DC designed and performed mass spectrometry and Edman sequencing experiments and data analysis. SW generated most of the constructs used in this study. GS conceived the project, analysed data and wrote the manuscript.

**Data and materials availability:** The raw mass spectrometry proteomics data have been deposited to the ProteomeXchange Consortium (<http://proteomecentral.proteomexchange.org>) via the PRIDE partner repository with the dataset identifier PXD001711.

**Competing interests:** The authors declare that they have no competing interests.

target many proteins for deubiquitylation, including TNF receptor-associated factors 3/6 (TRAF3/6) (11), estrogen receptor  $\alpha$  (ER $\alpha$ ) (12), the tumor suppressor protein p53 (13), and the cellular inhibitor of apoptosis c-IAP1 (14). Unlike other DUBs, several studies have described a non-canonical mode of OTUB1 action through which it inhibits the ubiquitylation of target proteins by binding to and inhibiting the E2 ubiquitin-conjugating enzymes independently of its catalytic activity (8-10). The non-canonical mode of action of OTUB1 has been reported to inhibit DNA damage repair and promote TGF $\beta$  signalling pathways (15, 16).

The precise molecular details of how OTUB1 imparts such diverse cellular roles remain to be defined. In the TGF $\beta$  pathway, OTUB1 is recruited only to phosphorylated, active SMAD2 and SMAD3 transcription factors (16, 17). Such phosphorylation-dependent recruitment of OTUB1 to its other targets may also be likely. Alternatively, phosphorylation or other posttranslational modifications within OTUB1 could alter its activity, ability to interact with its targets or regulators, and its subcellular localization. However, few studies have probed how posttranslational modifications within OTUB1 regulate its cellular functions.

In the course of a proteomic analysis on OTUB1, we identified potential phosphorylation modifications at Ser<sup>16</sup> and Ser<sup>18</sup> at the N-terminus of OTUB1 (16). Ser<sup>16</sup> and Ser<sup>18</sup> lie proximally to the domain resembling the ubiquitin interacting motif of OTUB1, which is essential for the non-canonical mode of action (8-10). Other global phosphoproteomic studies have also noted Ser<sup>16</sup> and Ser<sup>18</sup> on OTUB1 as phospho-modified residues, although the kinase(s) involved and the roles of these phosphorylation events remained to be defined (18-21). The residues surrounding Ser<sup>16</sup> of OTUB1, **GSDSEGVN**, with acidic residues at +1 and +3, make it an optimal site for phosphorylation by protein kinase CK2 (22-24). CK2 (derived from the misnomer casein kinase 2) is a ubiquitously expressed and highly pleiotropic protein kinase. The CK2 holoenzyme is a tetrameric complex comprising two regulatory  $\beta$ -subunits and two catalytic ( $\alpha$ ,  $\alpha'$  or  $\alpha''$  splice variants) subunits in a homomeric or heteromeric conformation. In cells, the subunits can exist individually or as the holoenzyme (22, 23, 25). CK2 is a constitutively active kinase and the basal catalytic activity is not influenced by specific ligands, extracellular stimuli or metabolic conditions. The phosphorylation of CK2 substrates is individually regulated through different conformations and regulated assembly of the holoenzyme and subunits, regulatory interactions with CK2 inhibitors or activators and through protein-protein interactions (24, 26, 27). CK2 phosphorylates over 300 substrates and therefore regulates many cellular processes (22, 28). CK2 regulates the function of deubiquitylating enzymes Ataxin-3 and OTUD5 through phosphorylation. Phosphorylation of Ataxin-3 by CK2 at Ser<sup>340</sup> and Ser<sup>352</sup> within its third ubiquitin-interaction motif promotes its nuclear localization, aggregation and stability (29). OTUD5 is catalytically activated upon phosphorylation by CK2 at Ser<sup>177</sup> (30).

Here, we investigated whether CK2 mediated the phosphorylation of OTUB1 at Ser<sup>16</sup> and what functional relevance this modification had in various cell types.

## Results

### CK2 phosphorylates OTUB1 at Ser<sup>16</sup> in vitro

A proteomic analysis on OTUB1 expressed in HEK293 cells identified a tryptic peptide corresponding to residues 11-36 (QEPLGSDSEGVNCLAYDEAIMAQQDR) with a phosphorylation modification, potentially at either Ser<sup>16</sup> or Ser<sup>18</sup> (fig. S1A). We set out to characterize the phosphorylation of OTUB1 at Ser<sup>16</sup> and Ser<sup>18</sup> in vitro and in vivo. Because residues surrounding Ser<sup>16</sup> of OTUB1 (GSDSEGVN) conform to a putative CK2 phosphomotif [acidic residue at +1 and +3 positions (22)], we set up in vitro kinase assays with OTUB1 and CK2 $\alpha$  as well as a panel of other Ser/Thr protein kinases (Fig. 1A). All of these kinases were verified as being active toward their respective peptide substrates and were used previously for kinase profiling screens (31). Only CK2 $\alpha$ , but not CaMK1 $\alpha/\beta$ , NUAK1/2, GSK3 $\beta$ , Aurora A, B, and C and PLK1, phosphorylated OTUB1 robustly in vitro (Fig. 1A). The precise CK2 $\alpha$  phosphorylation site on OTUB1 was determined by a combination of mass spectrometry and solid-phase Edman sequencing. In the first method, phosphorylated OTUB1 from the CK2 $\alpha$  kinase assay using  $\gamma^{32}\text{P}$ -ATP in vitro was excised from the gel, trypsin-digested, and separated by chromatography on a C<sub>18</sub> column. From this, a single  $\gamma^{32}\text{P}$ -labelled peak eluting at 25% acetonitrile was identified (Fig. 1B). Analysis of this peptide by mass spectrometry resulted in a mass to charge (m/z) ratio of 2975.2314, which is identical to that of the OTUB1 tryptic peptide (QEPLGSDSEGVNCLAYDEAIMAQQDR) with an additional single phosphorylation modification. This suggested that the phosphorylation occurred on only one of three Ser or Tyr residues present within this peptide. To identify the phosphorylation modified residue, the peptide was subjected to solid-phase Edman degradation.  $\gamma^{32}\text{P}$  radioactivity was released after the sixth cycle of Edman degradation, suggesting that CK2 $\alpha$  phosphorylates OTUB1 only at Ser<sup>16</sup> (Fig. 1C). Consistent with these findings, CK2 $\alpha$  failed to phosphorylate OTUB1[S16A] and OTUB1[S16A/S18A] mutants but not OTUB1[S18A] in vitro (Fig. 1D).

The active CK2 can exist as a CK2 $\alpha$  catalytic subunit monomer or a CK2 $\alpha$  and non-catalytic CK2 $\beta$  subunit holoenzyme. Class I CK2 substrates can be phosphorylated by both CK2 $\alpha$  catalytic subunit and the holoenzyme, whereas class II substrates can only be phosphorylated by the CK2 $\alpha$  subunit and not the holoenzyme (25). OTUB1 conforms to class I CK2 substrates because both the CK2 $\alpha$  catalytic subunit alone (Fig. 1D) and the CK2 $\alpha/\beta$  holoenzyme (Fig. 1E) phosphorylated OTUB1 in vitro. We generated an antibody against pSer<sup>16</sup>-OTUB1 and it recognized wild-type phosphorylated OTUB1, but not OTUB1[S16A], when incubated in vitro with CK2 $\alpha$  (Fig. 1F).

### The type I TGF $\beta$ receptor ALK5 phosphorylates OTUB1 at Ser<sup>18</sup> in vitro

The analysis of the CK2 consensus motif surrounding Ser<sup>16</sup> within OTUB1 reveals that phosphorylation of Ser<sup>18</sup> at +2 position (GSDSEGVN) could improve CK2 catalysis at Ser<sup>16</sup> (22). Consistent with this notion, we found that the phospho-Ser<sup>18</sup> derivative OTUB1 peptide (RRRKQEPLGSDSEGVN) appears to be a substantially better substrate for the CK2 holoenzyme than the native non-phospho OTUB1 peptide (RRRKQEPLGSDSEGVN), with lower K<sub>m</sub> and higher V<sub>max</sub> values observed for phospho over non-phospho peptide (Fig. 2A). These observations imply that potential Ser<sup>18</sup> phosphorylation in cells could

promote a substrate-level increase of Ser<sup>16</sup> phosphorylation by CK2 by improving the consensus sequence. Furthermore, in our phosphoproteomic analysis of OTUB1 when overexpressed in HEK293 cells, we observed a two-fold increase in the phosphorylation of the identified OTUB1 phosphopeptide (QEPLGSDSEGVNCLAYDEAIMAQDR) upon TGFβ stimulation (fig. S1A). TGFβ and BMP ligands trigger the activation of the type I TGFβ/BMP receptors (also known as ALKs), which are Ser/Thr protein kinases that phosphorylate R-SMAD transcription factors at their SXS motif (32). Because Ser<sup>16</sup> and Ser<sup>18</sup> loosely conform to the ALK phosphorylation SXS motif found in R-SMADs, we investigated whether ALKs could phosphorylate OTUB1 at Ser<sup>16</sup> and/or Ser<sup>18</sup> in vitro. ALK2 through ALK6 all phosphorylated OTUB1 in vitro; however the TGFβ-activated ALK4 and ALK5 phosphorylated OTUB1 more robustly than the BMP-activated ALK2, ALK3 and ALK6 (Fig. 2B). SB505124, a selective inhibitor of TGFβ-activated ALKs, inhibited the phosphorylation of OTUB1 by ALK5 in a dose-dependent manner (Fig. 2C). The stoichiometry of its phosphorylation by ALK5 in vitro was comparable to that of its *bona fide* substrates SMAD2 and SMAD3 (Fig. 2D). Furthermore, upon co-expression in HEK293 cells, OTUB1 interacted with ALK5 (fig. S1B). In order to investigate whether Ser<sup>16</sup> and Ser<sup>18</sup> were targeted for phosphorylation by ALK5, we set up an in vitro kinase assay with OTUB1, OTUB1[S16A], OTUB1[S18A] and OTUB1[S16/18A] as substrates for ALK5. Both OTUB1 and OTUB1[S16A] were robustly phosphorylated by ALK5 (Fig. 2E), suggesting that Ser<sup>16</sup> was not a major ALK5 phosphorylation site. In contrast, OTUB1[S18A] was poorly phosphorylated by ALK5, whereas OTUB1[S16A/S18A] was not phosphorylated (Fig. 2E), suggesting that Ser<sup>18</sup> is the main ALK5 phosphorylation site on OTUB1. Our attempts to generate an antibody against pSer<sup>18</sup>-OTUB1 failed repeatedly and consequently we have been unable to establish whether TGFβ induces the phosphorylation of endogenous OTUB1 at Ser<sup>18</sup> in cells. Nonetheless, we exploited ALK5-null MEFs (33), in which TGFβ fails to induce SMAD2 phosphorylation, to investigate whether the phosphorylation of Ser<sup>16</sup> was affected by TGFβ-induction. The abundance of pSer<sup>16</sup>-OTUB1 was almost identical in wild-type and ALK5-null MEFs upon TGFβ induction. The restoration of wild-type ALK5 in ALK5<sup>-/-</sup> MEFs restored TGFβ-induced SMAD2 phosphorylation, whereas expression of the empty vector or catalytically inactive ALK5 did not (Fig. 2F). Under these conditions, the pSer<sup>16</sup>-OTUB1 abundance remained unchanged (Fig. 2F). Similarly TGFβ, BMP and Activin A did not substantially enhance the phosphorylation of HA-OTUB1 at Ser<sup>16</sup> compared to controls (fig. S1C). These findings suggest that TGFβ ligands are unlikely to induce the phosphorylation of Ser<sup>18</sup> sufficiently to impact the phosphorylation of Ser<sup>16</sup> in cells. Therefore, if the phosphorylation of Ser<sup>18</sup> does indeed prime OTUB1 for enhanced phosphorylation of Ser<sup>16</sup> by CK2 in cells, the kinase(s) and signal(s) that mediate the phosphorylation of Ser<sup>18</sup> remain to be identified.

### OTUB1 is a *bona fide* substrate for CK2

To test whether OTUB1 is a *bona fide* substrate of CK2 in cells, the phosphorylation of OTUB1 at Ser<sup>16</sup> was further investigated by using pharmacological and genetic tools to inhibit CK2 in HEK293 cells. TDB (1-(β-D-2'-deoxyribofuranosyl)-4,5,6,7-tetrabromo-1H-benzimidazole), which has been reported as a cell-permeable selective inhibitor of CK2 (34), efficiently inhibited the phosphorylation of known CK2 targets, protein kinase AKT1 at Ser<sup>129</sup> and molecular chaperone protein CDC37 at Ser<sup>13</sup>, in a dose-dependent manner (35,

36) (fig. S2A). Treatment of cells with TDB decreased the phosphorylation of endogenous OTUB1 at Ser<sup>16</sup> to below detection in comparison to amount observed under control conditions by immunoblotting (Fig. 3A). Compared to controls, the detection of pSer<sup>16</sup>-OTUB1 and total OTUB1 was also decreased when cells were transfected with *OTUB1* siRNA (Fig. 3A). In addition to CK2, TDB inhibits 3 other kinases, namely PIM1, CLK2 and DYRK1A (37). However, none of these kinases phosphorylated OTUB1 in vitro (fig. S2B). Furthermore, quinalizarin, an inhibitor of CK2 that does not target PIM1 or DYRK1A (38), also inhibited the phosphorylation of endogenous OTUB1 at Ser<sup>16</sup> (Fig. 3B). Several other cell-permeable CK2 inhibitors are available, but the majority of them are less selective than TDB and quinalizarin (39-41).

To further confirm that CK2 was the mediator for OTUB1 Ser<sup>16</sup> phosphorylation in cells, a loss-of-function experiment was employed. Two *CK2* siRNAs (#1 and #3) that yielded a robust CK2 knockdown both resulted in the depletion of Ser<sup>16</sup> phosphorylation of HA-OTUB1 in HEK293 cells (Fig. 3C). Furthermore, the depletion of endogenous pSer<sup>16</sup>-OTUB1 caused by *CK2* siRNA was partially rescued by restoration with FLAG-CK2 $\alpha$  (Fig. 3D), ruling out any off-target effects of *CK2* siRNA. A gain-of-function experiment with wild type CK2 $\alpha$  and CK2 $\alpha$ '<sup>+</sup>, but not catalytically inactive CK2 $\alpha$ [D156A] mutant, in HEK293 cells resulted in enhanced amounts of endogenous pSer<sup>16</sup>-OTUB1 (Fig. 3E). Collectively, these experiments indicate that OTUB1 is a *bona fide* substrate for CK2 in cells. Interestingly, when we analyzed the distribution of pSer<sup>16</sup>-OTUB1 in mouse tissues, its abundance appeared to correlate with the presence of CK2 $\alpha$ , with highest amounts observed in the brain and thymus (Fig. 3F).

### Phosphorylation of OTUB1 at Ser<sup>16</sup> does not affect its catalytic activity and interactions with UBE2N

Having established OTUB1 as a substrate for CK2 in vitro and in vivo, we proceeded to investigate the molecular roles of pSer<sup>16</sup>-OTUB1. OTUB1 deubiquitylates K48-linked ubiquitin chains and its deubiquitylase activity is enhanced by E2 enzymes (7). To investigate whether phosphorylation of OTUB1 by CK2 affects OTUB1 DUB activity, we set up a time course of deubiquitylation with OTUB1 and CK2-phosphorylated OTUB1 using K48-linked di-ubiquitin molecules as substrates (Fig. 4A). Deubiquitylation was observed in the absence and presence of UBE2D2 and the phosphorylation of OTUB1 at Ser<sup>16</sup> did not substantially alter its catalytic activity (Fig. 4A). OTUB1 exclusively cleaves K48-linked ubiquitin chains (1), therefore we tested whether Ser<sup>16</sup> phosphorylation alters the ability of OTUB1 to cleave other ubiquitin chain linkages. Whereas pSer<sup>16</sup>-OTUB1 cleaved K48-linked di-ubiquitin chains, it was unable to cleave K6-, K11-, K27-, K29-, K33-, K63-, and M1-linked di-ubiquitin chains in vitro (Fig. 4B). Ser<sup>16</sup> lies proximal to the domain resembling the ubiquitin interaction motif at the N-terminus of OTUB1 (8, 9). Therefore, we tested whether Ser<sup>16</sup> phosphorylation alters the ability of OTUB1 to interact with ubiquitin chains. Whereas GST-OTUB1 robustly interacted with K63-linked polyubiquitin chains, no significant change in affinity was observed with the phospho-deficient mutant [S16A] and phospho-mimetic mutant [S16E] of GST-OTUB1 (Fig. 4C). Furthermore, immobilized K63-linked polyubiquitin chains but not monoubiquitin pulled down endogenous OTUB1 from HEK293 cell extracts treated with or without TDB (fig.

S3A). Under conditions in which K48-linked polyubiquitin chains bound to GST-WRNIP1 (Werner helicase interacting protein 1) (42), employed as a positive control, GST-OTUB1 or any of the mutants did not interact with K48-linked polyubiquitin chains (fig. S3B). OTUB1 inhibits E2 enzymes, including UBE2N, by interacting with them (8, 9, 15, 16). We tested the potential impact of Ser<sup>16</sup> phosphorylation on the ability of OTUB1 to interact with endogenous UBE2N. Wild type HA-OTUB1, which is phosphorylated at Ser<sup>16</sup>, expressed in HEK293 cells interacts robustly with endogenous UBE2N, whereas the N mutant of OTUB1 that lacks the first 47 amino acid residues does not (Fig. 4D). Treatment of cells with TDB, which inhibits Ser<sup>16</sup> phosphorylation, did not substantially alter the ability of OTUB1 to interact with UBE2N (Fig. 4D). Similarly, OTUB1 phosphomutants [S16A], [S18A] and [S16A/S18A] did not substantially alter the ability of OTUB1 to interact with UBE2N (Fig. 4D).

### Phosphorylation of OTUB1 at Ser<sup>16</sup> causes nuclear accumulation of OTUB1

Although OTUB1 has targets that reside in the nucleus and cytoplasm, the molecular mechanisms that control its subcellular localization are undefined. Because phosphorylation of proteins can alter their subcellular localization, we queried whether Ser<sup>16</sup> phosphorylation could alter that of OTUB1. Using immunofluorescence, we detected wild-type HA-OTUB1 mainly in the cytoplasm when expressed in U2OS cells (Fig. 5A). However, pSer<sup>16</sup>-OTUB1 was detected in the nucleus but not in the cytoplasm, where the majority of OTUB1 was detected (Fig. 5A). Treatment of cells with TDB, which inhibits Ser<sup>16</sup> phosphorylation, led to complete nuclear exclusion of both pSer<sup>16</sup>-OTUB1 and OTUB1 (Fig. 5A), suggesting that only pSer<sup>16</sup>-OTUB1 accumulates in the nucleus. Consistent with these observations, non-phosphorylatable mutant HA-OTUB1[S16A] expressed in U2OS cells was detected entirely in the cytoplasm, whereas the phosphomimetic mutant HA-OTUB1[S16E] expressed in U2OS cells was localized almost exclusively to the nucleus (Fig. 5B and fig. S4). At the endogenous level, in U2OS cells pSer<sup>16</sup>-OTUB1 was also detected in the nucleus, whereas total OTUB1 was detected in both the nucleus and cytoplasm (Fig. 5C). siRNA-mediated depletion of OTUB1 resulted in the loss of fluorescence of both pSer<sup>16</sup>-OTUB1 and OTUB1 (Fig. 5C). Treatment of cells with CK2 inhibitors quinalizarin and TDB decreased the amount of pSer<sup>16</sup>-OTUB1 and OTUB1 fluorescence in the nucleus compared to untreated controls (Fig. 5C). In two other cell lines, HeLa and HEK293, endogenous pSer<sup>16</sup>-OTUB1 was also only detected in the nuclear fractions, whereas OTUB1 was detected in both the nuclear and cytoplasmic fractions, but predominantly in the latter (Fig. 5D). In these cells unlike pSer<sup>16</sup>-OTUB1, CK2-mediated Ser<sup>129</sup> phosphorylated AKT was detected exclusively in the cytoplasmic fractions, whereas AKT was detected mainly in the cytoplasmic fraction but also in the nuclear fraction (Fig. 5D). CK2 $\alpha$  was detected primarily in the cytoplasmic fraction although some was also detected in the nuclear fraction (Fig. 5D). Glyceraldehyde-3-phosphate dehydrogenase (GAPDH) and Lamin A/C, used as controls, were detected in the cytoplasmic and nuclear fractions respectively (Fig. 5D).

To explore the mechanisms of nuclear/cytoplasmic shuttling of pSer<sup>16</sup>-OTUB1, U2OS cells were treated with leptomycin B, which inhibits exportin CRM1-dependent nuclear export (43), and importazole, which inhibits importin- $\beta$ -dependent nuclear import (44). Compared to control, the treatment of cells with leptomycin B did not substantially alter the abundance

of nuclear pSer<sup>16</sup>-OTUB1, suggesting that CRM1 might not be involved in the nuclear export of OTUB1 (fig. S5). When cells were treated with importazole, there was a slight increase in the amounts of pSer<sup>16</sup> and total OTUB1 in the nucleus compared to control (fig. S5), suggesting that although importazole does not inhibit the nuclear localization of pSer<sup>16</sup>-OTUB1, it is possible that it might exclude the nuclear entry of a key pSer<sup>16</sup>-OTUB1 phosphatase or factors that potentially regulate the nuclear exit of OTUB1. Without identifiable import/export signals within the OTUB1 sequence, it is hard to predict the precise mechanisms by which nuclear import/export of OTUB1 is achieved.

### Phosphorylation of OTUB1 at Ser<sup>16</sup> impacts IR-induced DNA-damage repair

OTUB1 prevents the ubiquitylation of chromatin through its association with and inhibition of UBE2N to inhibit repair of IR-induced DNA double strand breaks (DSBs) (15). We tested whether the phosphorylation of OTUB1 at Ser<sup>16</sup>, which alters its subcellular localization, was essential for the ability of OTUB1 to modulate IR-induced DNA damage repair. DSBs are recognized rapidly by the DNA-damage response pathways involving proteins such as protein kinase ATM and ring finger E3 ubiquitin ligases RNF8 and RNF168 that promote the recruitment of the RAP80 (retinoid × receptor interacting protein)–BRCA1 (breast cancer 1, early onset) complex and 53BP1 (p53 binding protein 1) to the sites of DNA damage to promote repair. As reported previously (15), we too observed that overexpression of wild-type HA-OTUB1 in U2OS cells resulted in the inhibition of 53BP1 foci formation in response to IR-induced DNA damage when compared to HA-empty vector control (Fig. 6, A and B). Similar to the wild-type HA-OTUB1, the overexpression of the phospho-deficient mutant HA-OTUB1[S16A] predominantly localized to the cytoplasm and impaired 53BP1 foci formation upon IR-induced DNA damage in U2OS cells (Fig. 6, A and B). In contrast, the overexpression of the phosphomimetic HA-OTUB1[S16E] mutant, which primarily localized to the nucleus, did not substantially alter the number of 53BP1 foci formation upon IR irradiation in U2OS cells (Fig. 6, A and B). These results suggest that nuclear localization of OTUB1 may be necessary for DSB-induced 53BP1 foci formation. Consistent with this notion, treatment of U2OS cells with TDB, which inhibited the phosphorylation of OTUB1 at Ser<sup>16</sup> and caused its nuclear exclusion, also impaired 53BP1 foci formation upon IR irradiation (Fig. 6, C and D).

### Discussion

In this study, we demonstrated that CK2 phosphorylated OTUB1 at Ser<sup>16</sup> in vitro and in cells, making OTUB1 a *bona fide* substrate for CK2. Our findings show that the phosphorylation of OTUB1 at Ser<sup>16</sup> did not impact its catalytic activity and its ability to interact with K63-linked ubiquitin chains as well as the E2 enzyme, UBE2N. Instead, we demonstrated that Ser<sup>16</sup> phosphorylation of OTUB1 was essential for its nuclear accumulation, suggesting that nuclear roles of OTUB1 are likely to be regulated through CK2-mediated phosphorylation of OTUB1. We further demonstrated that the nuclear accumulation of OTUB1 plays an important role in DNA DSB signalling.

Several proteomic studies, including ours, have identified Ser<sup>16</sup> and Ser<sup>18</sup> as potential phosphorylation sites within OTUB1 (16, 18-21). Until now, no reports showed whether and

how these sites on OTUB1 were phosphorylated at the endogenous level. On the basis of the sequence motif surrounding Ser<sup>16</sup> of OTUB1, we postulated that CK2 could phosphorylate Ser<sup>16</sup>. Indeed, we provided biochemical, pharmacological and genetic evidence to establish that CK2 phosphorylates OTUB1 at Ser<sup>16</sup>. Although not absolutely necessary, the phosphorylation of OTUB1 at Ser<sup>18</sup> makes OTUB1 a better substrate for CK2 to phosphorylate at Ser<sup>16</sup> in vitro. Whereas the evidence for phosphorylation of Ser<sup>18</sup> in cells and the potential kinase(s) mediating it remain to be identified, establishing this could imply a substrate-level regulation of Ser<sup>16</sup> phosphorylation by CK2 through a hierarchical mechanism. Better tools to recognize OTUB1 when phosphorylated at Ser<sup>18</sup> as well as at both Ser<sup>16</sup> and Ser<sup>18</sup> simultaneously are required to investigate this further.

Our findings suggest that the in vitro K48-DUB activity of OTUB1 and its association with K63-linked polyubiquitin and UBE2N are not affected by CK2-mediated Ser<sup>16</sup> phosphorylation, per our assay conditions. Although OTUB1 cleaves K48-linked ubiquitin chains, we were unable to detect robust interactions between wild-type OTUB1 or Ser<sup>16</sup> mutants and K48-ubiquitin chains in vitro, suggesting the interaction could be transient. A robust interaction assay is needed to test whether Ser<sup>16</sup> phosphorylation impacts the ability of OTUB1 to transiently interact with K48-linked ubiquitin chains.

The observation that the phosphorylation of OTUB1 at Ser<sup>16</sup> induced its nuclear accumulation suggests that its subcellular localization is regulated through phosphorylation. This is particularly important for DUBs, such as OTUB1, because they are known to target many substrates in different subcellular compartments, and understanding how they are recruited to their targets is key to being able to selectively target DUBs using therapeutics. It is not yet clear whether the function of OTUB1 on all its nuclear substrates relies on its phosphorylation at Ser<sup>16</sup>. CK2 is a constitutively active kinase that is localized in both nuclear and cytoplasmic compartments. Although CK2 appears to be mainly cytoplasmic, the majority of OTUB1 that is observed in the cytoplasm is not phosphorylated at Ser<sup>16</sup>. This raises the possibility that CK2-mediated phosphorylation of OTUB1 is a regulated process. One possible explanation is that a putative pSer<sup>16</sup>-OTUB1 phosphatase is active in the cytoplasm. Additionally, a nuclear pSer<sup>16</sup>-OTUB1 phosphatase could dynamically induce nuclear clearance of OTUB1. However, we have not yet identified potential phosphatase(s) that target pSer<sup>16</sup>-OTUB1 either in the cytoplasm or nucleus.

Physiologically, the nuclear accumulation of OTUB1 appears to be essential for the recruitment of 53BP1 to sites of DSBs. Overexpression of OTUB1 prevents the ubiquitylation of chromatin through its association with and inhibition of UBE2N to inhibit DNA DSB repair (15). We, too, observed that overexpression of OTUB1 and or the OTUB1[S16A] mutant, which primarily accumulated in the cytoplasm, severely inhibited IR-induced 53BP1 foci formation. However, the overexpression of the nuclear phosphomimetic OTUB1[S16E] mutant did not inhibit the IR-induced 53BP1 foci formation. Mutating Ser<sup>16</sup> to a non-phosphorylatable residue (S16A) or treating cells with TDB to block Ser<sup>16</sup> phosphorylation did not substantially affect the ability of OTUB1 to interact with UBE2N. It is possible that nuclear exclusion of overexpressed OTUB1 and OTUB1[S16A] mutants could have caused the nuclear exclusion of UBE2N or other OTUB1-interacting key DSB repair factors, thus resulting in defective DNA-damage

response signalling. However, the fact that overexpressed OTUB1[S16E] in the nucleus that can still interact with UBE2N does not inhibit IR-induced DNA DSB repair implies that the precise roles of OTUB1 in DNA DSB repair are still unresolved. Inhibition of CK2 by TDB, which also causes nuclear exclusion of OTUB1 through inhibition of Ser<sup>16</sup> phosphorylation, also resulted in defective 53BP1 recruitment to the sites of DNA-damage, further suggesting that nuclear accumulation of OTUB1 may be essential for proper DNA-damage repair. However, it should be noted that CK2 phosphorylates many other proteins that may also impact DNA damage repair signalling (45, 46). The use of CK2 inhibitors in *OTUB1*-null cells, which we have failed to generate thus far, could provide key molecular mechanisms underpinning the links between CK2 and OTUB1 in mediating DNA-damage responses. In *OTUB1*-null cells, it would be interesting to investigate whether the phosphomimetic OTUB1[S16E] mutant rescues the impact of TDB on DNA-damage repair. Given our observations that TDB appears to inhibit IR-induced DNA DSB repair, it would be interesting to investigate whether it sensitizes cells to other types of DNA damage insults.

We previously reported that the active, phosphorylated SMAD2/3/4 transcription complex recruits endogenous OTUB1 in response to TGF $\beta$  (16). This activated transcription complex also accumulates in the nucleus upon TGF $\beta$  stimulation. Here we found that OTUB1 can also localize to the nucleus upon phosphorylation of Ser<sup>16</sup>. Understanding the mechanisms by which the function of OTUB1 on its nuclear targets is regulated through its phosphorylation at Ser<sup>16</sup> could provide novel therapeutic insights. For example, the phosphorylation of OTUB1 at Ser<sup>16</sup> and Ser<sup>18</sup>, by unknown kinases, promotes cellular susceptibility to *Yersinia enterocolitica* and *pseudotuberculosis* infection (18). Now that we have established that CK2 phosphorylates OTUB1 at Ser<sup>16</sup>, it would be interesting to explore whether small molecule inhibitors of CK2 potentially decrease the infection of host cells by *Yersinia*. However, these future investigations should keep in mind that CK2 can phosphorylate over 300 proteins and off-target effects of CK2 inhibition are likely.

## Materials and Methods

### Cell culture and reagents

HEK293, U2OS and HeLa cells were cultured in DMEM (Gibco) supplemented with 10% FBS (Hyclone), 2 mM L-Glutamine (Lonza) and 1% penicillin/streptomycin (Lonza) and maintained at 37°C in a humidified atmosphere with 5% CO<sub>2</sub>. MEFs and H29 cells were cultured as described in the transfection methodology below. Human recombinant BMP2, TGF $\beta$ 1 or Activin A (R&D Systems) were resuspended in 4 mM HCl, 0.1% BSA. Cells were serum-starved for 16 hours at 37°C prior to ligand treatment with human recombinant BMP2 (25 ng/ml), TGF $\beta$ 1 (50 pM) or Activin A (20 ng/ml) for 1 hour. SB505124 (Sigma), a specific inhibitor of the TGF $\beta$  receptors ALK4, ALK5 and ALK7, was used at 1  $\mu$ M for 1 hour; and LDN198193 (Stemgent), an inhibitor of the BMP receptors ALK2, ALK3 and ALK6, was used at 100 nM for 1 hour (31). TDB and quinalizarin (CK2 inhibitors) (37, 38) were used at 10  $\mu$ M for 4 hours. To inhibit importin- $\beta$ -dependent nuclear import, importazole (Sigma) was used at 40  $\mu$ M for 4 hours, and to inhibit CRM1-dependent nuclear export, leptomycin B (Sigma) was used at 10  $\mu$ M for 4 hours. DNA-double strand breaks were induced by 5 Gy of ionizing radiation.

## Cell transfections

Plasmid transfections in HEK293 cells were performed with 25  $\mu$ l of polyethylenimine (1 mg/ml; Polysciences) in 25 mM HEPES pH7.5 in 1 ml DMEM and 2  $\mu$ g plasmid DNA (47). Plasmid transfections in U2OS cells were performed with 30  $\mu$ l of hyperfect (Qiagen) in 1 ml OptiMEM (Life Technologies) with 2  $\mu$ g plasmid DNA. After incubating for 15 min, the solution was added to U2OS or HEK293 cells, which were lysed 48 hours later.

All plasmids expressing mammalian proteins were cloned into pCMV5, with N-terminal FLAG or hemagglutinin (HA) tags. All DNA constructs used were verified by DNA sequencing, performed by DNA Sequencing & Services (MRCPPU, College of Life Sciences, University of Dundee, Scotland, [www.dnaseq.co.uk](http://www.dnaseq.co.uk)) using Applied Biosystems Big-Dye Ver 3.1 chemistry on an Applied Biosystems model 3730 automated capillary DNA sequencer.

For siRNA oligonucleotide transfections, the cells were transfected during attachment. 30  $\mu$ l transfectin (BioRad) and 300 pM of siRNA (per 10 cm diameter dish) were mixed in 2 ml OptiMEM. After incubating for 15 min, the solution was added to the cells and cells were lysed 48 hours post-transfection. The following siRNA oligonucleotides were used: *CK2* (#1) 5'-3': GCUGGUCGCUUACAUCACU (Dharmacon); *CK2* (#3) 5'-3': AACAUUGUCUGUACAGGUU (Dharmacon); *OTUB1* 5'-3': GCAAGUUCUUCGAGCACUU (Sigma); *FOXO4* (control) 5'-3': CCCGACCAGAGAUCGCUAA (Dharmacon).

Transformed *ALK5*<sup>-/-</sup> MEF cells were a kind gift of G. Inman (Dundee). A retroviral system was used to generate put backs (control, WT or kinase dead ALK5) in *Alk5*<sup>-/-</sup> MEF cells. H29 cells were cultured in growth media supplemented with doxycycline (20 ng/ml; Sigma), puromycin (2  $\mu$ g/ml; Sigma) and G418 (0.3 mg/ml; Sigma). The cells were grown to sub-confluency in a 15 cm dish and transfected using 75  $\mu$ l PEI in 2 ml DMEM and 25  $\mu$ g of plasmid DNA [pBABE-puro control, pBABE-puro *ALK5* or pBABE-puro *ALK5 D380A*]. Cells were transfected in 10 ml of growth medium supplemented with 1 % sodium pyruvate. After 48 hours, the virus containing media was filtered and added to 60% confluent *ALK5*<sup>-/-</sup> MEF cells in the presence of polybrene (8  $\mu$ g/ml; Sigma). Target cells were selected in growth media containing puromycin (2  $\mu$ g/ml) 24 hours post-viral infection.

## Cell lysis

For lysis, cells were scraped on ice in lysis buffer (50 mM Tris-HCl pH 7.5, 0.27 M sucrose, 150 mM NaCl, 1 mM EGTA, 1 mM EDTA, 1 mM sodium orthovanadate, 1 mM sodium  $\beta$ -glycerophosphate, 50 mM sodium fluoride, 5 mM sodium pyrophosphate, 1% Triton X-100, 0.5% Nonidet P-40) supplemented with complete protease inhibitors (1 tablet per 25 ml; Roche) and 0.1%  $\beta$ -mercaptoethanol (Sigma). Extracts were cleared and processed immediately or snap-frozen in liquid nitrogen and stored at -80°C. The protein concentration was determined with a photo spectrometer using Bradford protein assay reagent (Pierce) (48).

### Mouse tissue isolation

Tissues from mice were snap frozen in liquid nitrogen and ground with mortar and pestle. Pulverized tissues were resuspended in tissue lysis buffer (10 mM Tris/HCl pH 8, 150 mM NaCl, 1 mM EDTA, 1% NP40, 0.1% SDS, 1 tablet of complete protease inhibitors per 25 ml lysis buffer) and incubated on ice for 30 min before centrifugation. The cleared extracts were processed as described for cell extracts.

### Immunoprecipitation

Cleared cell extracts were mixed with Glutathione Sepharose beads (GE Healthcare), or FLAG- or HA-agarose beads (Sigma-Aldrich) for 2 hours at 4°C on a rotating platform. The beads were washed twice in lysis buffer containing 0.4 M NaCl, and twice in buffer A (50 mM Tris-HCl pH 7.5, 0.1 mM EGTA). IP and input samples were reduced in SDS sample buffer (62.5 mM Tris-HCl pH 6.8, 10% (v/v) glycerol, 2% (w/v) SDS, 0.02% (w/v) bromophenol blue, 5% (v/v)  $\beta$ -mercaptoethanol) and heated at 95°C for 5 min (16).

### SDS-PAGE and Western blotting

Reduced protein extracts (20  $\mu$ g of protein or 80  $\mu$ g for the detection of endogenous pSer<sup>16</sup>-OTUB1) or IPs were separated on 10% SDS-PAGE gels by electrophoresis and transferred to PVDF membranes (Millipore). Membranes were blocked in 5% (w/v) non-fat milk in TBS-T (50 mM Tris-HCl pH 7.5, 150 mM NaCl, 0.2% Tween-20), incubated overnight at 4°C in 5% milk-TBS-T or 3% BSA (bovine serum albumin)-TBS-T with the appropriate primary antibodies (all used at 1:1000 dilution from stocks, except for FLAG and GAPDH, which were used at 1:5000 dilution), followed by incubation with HRP-conjugated secondary antibodies (1:5000; obtained from Pierce) in 5% milk-TBS-T and detected by ECL luminescence (Thermo Scientific) (49).

### Antibodies

Antibodies against CK2 (ab10466), tubulin (ab176560), AKT1 pSer<sup>129</sup> (ab133458) and CDC37 pSer<sup>13</sup> (ab108360) were from Abcam. Antibodies against GAPDH (#2118), Lamin A/C (#2032), UBE2N (#6999), CDC37 (#3618) and AKT1 (#9272) were from Cell Signaling Technologies. The antibody against 53BP1 was from Bethyl Laboratories. The antibody against ubiquitin was from Dako (Z0458) and that against HA was from Roche (12CA5). HRP-conjugated antibodies against FLAG (#A8592) and HA (#12013819001) were from Sigma and Roche, respectively. Human recombinant full length OTUB1, ALK5 (amino acids 142-172) polypeptide, and pSer<sup>16</sup>-OTUB1 (amino acids 10-22, KQEPLGSDSEGVN) polypeptide were used as immunogens to generate the respective antibodies. All recombinant proteins, plasmids and antibodies generated for the present study are available on request and described in further detail on our reagents website (<https://mrcppureagents.dundee.ac.uk/>).

### In vitro kinase assay

To phosphorylate OTUB1 in vitro, 150 ng of kinase and 2  $\mu$ g of substrate were incubated in a total volume of 20  $\mu$ l kinase assay buffer (50 mM Tris/HCl pH 7.5, 0.1%  $\beta$ -mercaptoethanol, 0.1 mM EGTA, 10 mM MgCl<sub>2</sub>, 0.5  $\mu$ M Microcystin-LR and 0.1

mM  $\gamma$ - $^{32}\text{P}$ -ATP (500 cpm/pmole for routine autoradiography analysis; 10000 cpm/pmole for mapping phospho-residues) at 30°C for 30 min. The kinase assay was stopped by adding SDS sample buffer containing 1%  $\beta$ -mercaptoethanol and heating at 95°C for 5 min. The samples were resolved by SDS-PAGE and the gels were stained with Coomassie and dried (50). The radioactivity was analyzed by autoradiography. Films were developed using a Konica automatic developer.

### Identification of phosphorylated peptides

An in vitro kinase assay was performed to phosphorylate OTUB1, and the bands were excised, digested with trypsin and the peptides isolated and dried as described previously (50). The dried peptides were reconstituted in 5 % acetonitrile (ACN)/ 0.1 % trifluoroacetic acid (TFA) and injected into a 218TP5215 C<sub>18</sub> column equilibrated in 0.1% TFA, with a linear ACN gradient at a flow rate of 0.2 ml/minute and fractions of 100  $\mu$ l were collected. The major  $^{32}\text{P}$  eluting peptide was analyzed by an LTQ-orbitrap mass spectrometer (Thermo Scientific) equipped with a nanoelectrospray ion source (Thermo) and coupled to a Proxeon EASY-nLC system (Thermo). Peptides were injected onto a Thermo (Part No. 160321) Acclaim PepMap100 reverse phase C18 3 $\mu$ m column, 75 $\mu$ m  $\times$  15cm, with a flow of 300 nl/min and eluted with a 20 min linear gradient of 95% solvent A (2% Acetonitrile, 0.1% formic acid in H<sub>2</sub>O) to 40% solvent B (90% acetonitrile, 0.08% Formic acid in H<sub>2</sub>O), followed by a rise to 80%B at 23min. The instrument was operated with the “lock mass” option to improve the mass accuracy of precursor ions and data were acquired in the data-dependent mode, automatically switching between MS and MS-MS acquisition. Full scan spectra (m/z 340-1800) were acquired in the orbitrap with resolution R = 60,000 at m/z 400 (after accumulation to an FTMS Full AGC Target; 1,000,000; MSn AGC Target; 100,000). The 5 most intense ions, above a specified minimum signal threshold (5,000), based upon a low resolution (R = 15,000) preview of the survey scan, were fragmented by collision induced dissociation and recorded in the linear ion trap, (Full AGC Target; 30,000. MSn AGC Target; 5,000). Multi-Stage-Activation in the Mass Spectrometer was used to produce a pseudo MS3 scan of parent ions, allowing for a neutral loss of 48.9885, 32.6570, 24.4942, for 2+, 3+ and 4+ ions respectively, which should provide a better analysis of Phosphopeptides. The resulting pseudo MS3 scan was automatically combined with the relevant MS2 scan prior to data analysis by Mascot ([www.matrixscience.com](http://www.matrixscience.com)). To determine the phosphorylated residue in the  $^{32}\text{P}$ -labelled peptide, the peptides were also coupled covalently to a Sequelon-arylamine membrane (Applied Biosystems/Millipore) with N-(3-Dimethylaminopropyl)-N'-ethylcarbodiimide hydrochloride (Sigma, E1769) in 0.5M MES (2-(N-morpholino) ethanesulfonic acid) buffer pH 4.4 and subjected to Edman sequencing as previously described (51) except that a Shimadzu PPSQ33A sequencer was used; modified by the addition of a fraction collector to allow collection of the anilinothiazolinone-amino acid that was produced after each cleavage step of the normal sequencing cycle. The  $^{32}\text{P}$  radioactivity released after each Edman cycle was measured by Cerenkov counting of the eluate from each cycle.

### Kinetic analysis of CK2-mediated phosphorylation of OTUB1 peptides

CK2 $\alpha$  activity assays were carried out with 30 ng protein at 37°C in the presence of increasing concentrations of the OTUB1 peptide (RRRKQEPLGSDSEGVN) or pSer<sup>18</sup>.

OTUB1 peptide (RRRKQEPLGSDSEGVN) in a final volume of 25  $\mu$ l, containing 50 mM Tris-HCl pH 7.5, 100 mM NaCl, 10 mM MgCl<sub>2</sub>, 0.02 mM <sup>33</sup>P-ATP (~1000 cpm/pmol), as described previously (34). The reaction was started with the addition of the kinase and was stopped after 10 min by adding of 5  $\mu$ l of 0.5 M orthophosphoric acid before spotting aliquots onto phosphocellulose filters. Filters were washed in 75 mM phosphoric acid (5-10 ml/each) four times and then once in methanol and dried before counting. Kinetic constants were determined by double reciprocal plots, constructed from initial rate measurements fitted onto the Michaelis-Menten equation.

#### **K48-linked di-ubiquitin cleavage assay**

An in vitro kinase assay was set up with CK2 $\alpha$  and OTUB1 (maintaining 150 ng kinase: 2  $\mu$ g substrate ratio as described above) in kinase assay buffer (50 mM Tris/HCl pH 7.5, 0.1%  $\beta$ -mercaptoethanol, 0.1 mM EGTA, 10 mM MgCl<sub>2</sub>, 0.5  $\mu$ M Microcystin-LR) in the presence or absence of 0.1 mM ATP at 30°C for 30 min. Phosphorylated or unphosphorylated OTUB1 (0.5  $\mu$ M) was then incubated with K48-linked di-ubiquitin (5  $\mu$ M, Boston Biochem) in the presence or absence of UBE2D2 (15  $\mu$ M) in assay buffer (20 mM HEPES pH 7.5, 5 mM DTT, 100 mM NaCl) at 37°C as described previously (7). The reaction was stopped at indicated time points and the samples were resolved by SDS-PAGE, the gel was Coomassie stained or transferred to a PVDF membrane for immunoblotting.

#### **DUB assays on differently K-linked di-ubiquitins**

An in vitro kinase assay was set up with CK2 $\alpha$  and GST-OTUB1 substrate (as described above). Phosphorylated GST-OTUB1 (5  $\mu$ M) was then incubated with K6-, K11-, K27-, K29-, K33-, K48-, K63-, or M1-di-ubiquitin molecules (6.5  $\mu$ M, obtained from Y. Kulathu, Dundee) at 37°C in assay buffer (50 mM Tris/HCL pH 7.5, 5 mM DTT, 50 mM NaCl). The reaction was stopped at indicated time points and the samples were resolved by SDS-PAGE and the gel was Coomassie stained.

#### **K48- and K63-linked polyubiquitin binding assays**

GST, GST-OTUB1, GST-OTUB1[S16A] and GST-OTUB1[S16E] (0.05  $\mu$ g/ $\mu$ l) were individually incubated with K48- or K63-linked polyubiquitin chains (0.04  $\mu$ g/ $\mu$ l, Boston Biochem) for 60 min at 21°C in assay buffer (25 mM HEPES pH 7.5, 150 mM NaCl, 2 mM MgCl<sub>2</sub>, 0.5% Triton X-100, 1mM EGTA). GST pull-downs were performed as described above and resolved by SDS-PAGE for immunoblot analyses. For the endogenous interaction of OTUB1 with K63-linked polyubiquitin chains, beads that were coupled to mono-ubiquitin or K63-linked polyubiquitin chains (kind gift from S. Virdee, Dundee) were incubated for 1 hour at 4°C in lysates (1 mg protein) from HEK293 cells that was left untreated or treated with TDB (10  $\mu$ M for 4 h) in the presence of 20 mM Iodoacetamide (Sigma). The beads were washed twice in lysis buffer containing 0.4 M NaCl, and twice in buffer A (50 mM Tris-HCl pH 7.5, 0.1 mM EGTA). IP and input samples were reduced in SDS sample buffer (62.5 mM Tris-HCl pH 6.8, 10% (v/v) glycerol, 2% (w/v) SDS, 0.02% (w/v) bromophenol blue, 5% (v/v)  $\beta$ -mercaptoethanol) and heated at 95°C for 5 min.

## Immunofluorescence microscopy

Transfected U2OS cells were seeded onto poly-L-lysine treated glass cover slips in 6-well culture dishes and treated accordingly. Cells were washed in PBS before fixation with 4% paraformaldehyde for 10 min at room temperature (RT). The coverslips were washed a further three times before permeabilization of the cells with 0.5% NP-40 in PBS for 15 min at RT. Cells were rinsed with PBS before being incubated for 1 hour in blocking solution [5 % (v/v) normal donkey serum, 0.01 % (v/v) fish skin gelatin, 0.1 % (v/v) Triton X-100, 0.05 % (v/v) Tween-20 in PBS] (52). Primary antibody incubation was done for 16 hours in a humidified chamber at 4°C. After thorough washes in PBS, cells were incubated with AlexaFluor® secondary antibodies for 1 hour in the dark. Cells were washed three more times in PBS and once with deionised water before being mounted onto glass slides using ProLong® Gold mounting reagent (Life Technologies), which contained the nuclear stain 4', 6-diamidino-2-phenylindole (DAPI). Slides were viewed using a Leica microscope 510 fitted with a 40x lens and a cooled charge-coupled device (CCD) camera.

## Subcellular fractionation

Subcellular fractionations were performed using the NE-PER kit (Thermo Scientific) according to the manufacturer's instructions. The lysis buffers were supplemented with protease inhibitors (Roche) and phosphatase inhibitors (1.5 mM sodium orthovanadate, 50 mM sodium fluoride and 10 mM sodium pyrophosphate). Fractions were reduced in SDS sample buffer and 20 µg of protein from each fraction were resolved by SDS-PAGE as described above.

## Statistical analysis

All experiments have a minimum of three biological replicates. Data are presented as mean with error bars indicating the standard deviation. Statistical significance of differences between experimental groups was assessed using Student's *t*-test. Differences in mean were considered significant if  $P < 0.05$ . Data are annotated with \* for  $P < 0.05$ , \*\* for  $P < 0.01$  and \*\*\* for  $P < 0.001$ . All Western blots shown are representative of biological replicates.

## Supplementary Material

Refer to Web version on PubMed Central for supplementary material.

## Acknowledgements

We thank Yogesh Kulathu for providing us with di-ubiquitin chains, Satpal Virdee for immobilized ubiquitin chains, Gareth Inman and Stefan Karlsson for *ALK5*<sup>-/-</sup> MEFs, Kirsten McLeod and Janis Stark for help with tissue culture, the staff at the Sequencing Service (School of Life Sciences, University of Dundee, Scotland) for DNA sequencing and the protein production teams at the Division of Signal Transduction Therapy (DSTT; University of Dundee) coordinated by Hilary McLauchlan and James Hastie for the expression and purification of proteins and antibodies. We also thank Alex Knebel and Richard Ewan for OTUB1 expression and purification and Oriano Marin (CRIBI, University of Padova) for the synthesis of OTUB1 synthetic fragments. We thank Alejandro Rojas-Fernandez, Ivan Munoz, Polyxeni Bozatzki and the PRIDE team for technical assistance.

**Funding:** LAP is supported by Associazione Italiana per la Ricerca sul Cancro (AIRC) (grant IG-10312). LH is supported by the UK MRC Prize PhD studentship. GS is supported by the UK Medical Research Council and the pharmaceutical companies supporting the DSTT (AstraZeneca, Boehringer-Ingelheim, GlaxoSmithKline, Merck-Serono, Pfizer and Johnson & Johnson).

## References and Notes

1. Mevissen, Tycho E. T.; Hospenthal, Manuela K.; Geurink, Paul P.; Elliott, Paul R.; Akutsu, M.; Arnaudo, N.; Ekkebus, R.; Kulathu, Y.; Wauer, T.; El Oualid, F.; Freund, Stefan M. V.; Ovaa, H.; Komander, D. OTU Deubiquitinases Reveal Mechanisms of Linkage Specificity and Enable Ubiquitin Chain Restriction Analysis. *Cell*. 2013; 154:169–184. [PubMed: 23827681]
2. Komander D, Clague MJ, Urbe S. Breaking the chains: structure and function of the deubiquitinases. *Nature reviews. Molecular cell biology*. 2009; 10:550–563.
3. Balakirev MY, Tcherniuk SO, Jaquinod M, Chroboczek J. Otubains: a new family of cysteine proteases in the ubiquitin pathway. *EMBO Rep*. 2003; 4:517–522. [PubMed: 12704427]
4. Edelmann MJ, Iphöfer A, Akutsu M, Altun M, di Gleria K, Kramer HB, Fiebigler E, Dhe-Paganon S, Kessler BM. Structural basis and specificity of human otubain 1-mediated deubiquitination. *Biochemical Journal*. 2009; 418:379. [PubMed: 18954305]
5. Messick TE, Russell NS, Iwata AJ, Sarachan KL, Shiekhhattar R, Shanks JR, Reyes-Turcu FE, Wilkinson KD, Marmorstein R. Structural basis for ubiquitin recognition by the Otub1 ovarian tumor domain protein. *J Biol Chem*. 2008; 283:11038–11049. [PubMed: 18270205]
6. Wang T, Yin L, Cooper EM, Lai MY, Dickey S, Pickart CM, Fushman D, Wilkinson KD, Cohen RE, Wolberger C. Evidence for bidentate substrate binding as the basis for the K48 linkage specificity of otubain 1. *J Mol Biol*. 2009; 386:1011–1023. [PubMed: 19211026]
7. Wiener R, DiBello AT, Lombardi PM, Guzzo CM, Zhang X, Matunis MJ, Wolberger C. E2 ubiquitin-conjugating enzymes regulate the deubiquitinating activity of OTUB1. *Nature Structural and Molecular Biology*. 2013; 20:1033–1039.
8. Wiener R, Zhang X, Wang T, Wolberger C. The mechanism of OTUB1-mediated inhibition of ubiquitination. *Nature*. 2012; 483:612–622.
9. Juang YC, Landry MC, Sanches M, Vittal V, Leung CC, Ceccarelli DF, Mateo AR, Pruneda JN, Mao DY, Szilard RK, Orlicky S, Munro M, Brzovic PS, Klevit RE, Sicheri F, Durocher D. OTUB1 Co-opts Lys48-Linked Ubiquitin Recognition to Suppress E2 Enzyme Function. *Molecular cell*. 2012; 45:384–397. [PubMed: 22325355]
10. Sato Y, Yamagata A, Goto-Ito S, Kubota K, Miyamoto R, Nakada S, Fukai S. Molecular basis of Lys-63-linked polyubiquitination inhibition by the interaction between human deubiquitinating enzyme OTUB1 and ubiquitin conjugating enzyme UBC13. *J Biol Chem*. 2012; 287:25860–25868. [PubMed: 22679021]
11. Li S, Zheng H, Mao AP, Zhong B, Li Y, Liu Y, Gao Y, Ran Y, Tien P, Shu HB. Regulation of virus-triggered signaling by OTUB1- and OTUB2-mediated deubiquitination of TRAF3 and TRAF6. *J Biol Chem*. 2010; 285:4291–4297. [PubMed: 19996094]
12. Stanic V, Malovannaya A, Qin J, Lonard DM, O'Malley BW. OTU Domain-containing ubiquitin aldehyde-binding protein 1 (OTUB1) deubiquitinates estrogen receptor (ER) alpha and affects ERalpha transcriptional activity. *J Biol Chem*. 2009; 284:16135–16145. [PubMed: 19383985]
13. Sun X-X, Challagundla KB, Dai M-S. Positive regulation of p53 stability and activity by the deubiquitinating enzyme Otubain 1. *The EMBO journal*. 2011; 31:576–592. [PubMed: 22124327]
14. Goncharov T, Niessen K, de Almagro MC, Izrael-Tomasevic A, Fedorova AV, Varfolomeev E, Arnott D, Deshayes K, Kirkpatrick DS, Vucic D. OTUB1 modulates c-IAP1 stability to regulate signalling pathways. *EMBO J*. 2013; 32:1103–1114. [PubMed: 23524849]
15. Nakada S, Tai I, Panier S, Al-Hakim A, Iemura S.-i. Juang Y-C, O'Donnell L, Kumakubo A, Munro M, Sicheri F, Gingras A-C, Natsume T, Suda T, Durocher D. Non-canonical inhibition of DNA damage-dependent ubiquitination by OTUB1. *Nature*. 2010; 466:941–946. [PubMed: 20725033]
16. Herhaus L, Al-Salihi M, Macartney T, Weidlich S, Sapkota GP. OTUB1 enhances TGFβ signalling by inhibiting the ubiquitylation and degradation of active SMAD2/3. *Nature Communications*. 2013; 4:2519.
17. Herhaus L, Sapkota GP. The emerging roles of deubiquitylating enzymes (DUBs) in the TGFβ and BMP pathways. *Cell Signal*. 2014; 26:2186–2192. [PubMed: 25007997]

18. Edelmann MJ, Kramer HB, Altun M, Kessler BM. Post-translational modification of the deubiquitinating enzyme otubain 1 modulates active RhoA levels and susceptibility to *Yersinia* invasion. *FEBS Journal*. 2010; 277:2515–2530. [PubMed: 20553488]
19. Wagner SA, Beli P, Weinert BT, Nielsen ML, Cox J, Mann M, Choudhary C. A Proteome-wide, Quantitative Survey of In Vivo Ubiquitylation Sites Reveals Widespread Regulatory Roles. *Molecular & Cellular Proteomics*. 2011; 10
20. Kim W, Bennett Eric J, Huttlin Edward L, Guo A, Li J, Possemato A, Sowa Mathew E, Rad R, Rush J, Comb Michael J, Harper JW, Gygi Steven P. Systematic and Quantitative Assessment of the Ubiquitin-Modified Proteome. *Molecular cell*. 2011; 44:325–340. [PubMed: 21906983]
21. Pozuelo Rubio M, Geraghty KM, Wong BHC, Wood NT, Campbell DG, Morrice N, Mackintosh C. 14-3-3-affinity purification of over 200 human phosphoproteins reveals new links to regulation of cellular metabolism, proliferation and trafficking. *Biochem. J*. 2004; 379:395–408. [PubMed: 14744259]
22. Meggio F, Pinna LA. One-thousand-and-one substrates of protein kinase CK2? *The FASEB Journal*. 2003; 17:349–368.
23. Battistutta R, Lolli G. Structural and functional determinants of protein kinase CK2alpha: facts and open questions. *Mol. Cell. Biochem*. 2011; 356:67–73. [PubMed: 21739155]
24. Montenarh M. Cellular regulators of protein kinase CK2. *Cell Tissue Res*. 2010; 342:139–146. [PubMed: 20976471]
25. Pinna LA. Protein kinase CK2: a challenge to canons. *Journal of Cell Science*. 2002; 115:3873–3878. [PubMed: 12244125]
26. Pinna LA. The Raison D'Être of Constitutively Active Protein Kinases: The Lesson of CK2. *Accounts of Chemical Research*. 2003; 36:378–384. [PubMed: 12809523]
27. Litchfield DW. Protein kinase CK2: structure, regulation and role in cellular decisions of life and death. *The Biochemical journal*. 2003; 369:1–15. [PubMed: 12396231]
28. Ruzzene M, Pinna LA. Addiction to protein kinase CK2: A common denominator of diverse cancer cells? *Biochimica et Biophysica Acta (BBA) - Proteins and Proteomics*. 2010; 1804:499–504.
29. Mueller T, Breuer P, Schmitt I, Walter J, Evert BO, Wullner U. CK2-dependent phosphorylation determines cellular localization and stability of ataxin-3. *Human Molecular Genetics*. 2009; 18:3334–3343. [PubMed: 19542537]
30. Huang OW, Ma X, Yin J, Flinders J, Maurer T, Kayagaki N, Phung Q, Bosanac I, Arnott D, Dixit VM, Hymowitz SG, Starovasnik MA, Cochran AG. Phosphorylation-dependent activity of the deubiquitinase DUBA. *Nature Structural and Molecular Biology*. 2012; 19:171–175.
31. Vogt J, Traynor R, Sapkota GP. The specificities of small molecule inhibitors of the TGFs and BMP pathways. *Cell Signal*. 2011; 23:1831–1842. [PubMed: 21740966]
32. Al-Salihi MA, Herhaus L, Sapkota GP. Regulation of the transforming growth factor beta pathway by reversible ubiquitylation. *Open Biology*. 2012; 2:120082–120082. [PubMed: 22724073]
33. Larsson J, Goumans MJ, Sjostrand LJ, van Rooijen MA, Ward D, Leveen P, Xu X, ten Dijke P, Mummery CL, Karlsson S. Abnormal angiogenesis but intact hematopoietic potential in TGF-beta type I receptor-deficient mice. *The EMBO Journal*. 2001; 20:1663–1673. [PubMed: 11285230]
34. Cozza G, Sarno S, Ruzzene M, Girardi C, Orzeszko A, Kazimierczuk Z, Zagotto G, Bonaiuto E, Di Paolo ML, Pinna LA. Exploiting the repertoire of CK2 inhibitors to target DYRK and PIM kinases. *Biochimica et Biophysica Acta (BBA) - Proteins and Proteomics*. 2013; 1834:1402–1409.
35. Di Maira G, Salvi M, Arrigoni G, Marin O, Sarno S, Brustolon F, Pinna LA, Ruzzene M. Protein kinase CK2 phosphorylates and upregulates Akt/PKB. *Cell Death Differ*. 2005; 12:668–677. [PubMed: 15818404]
36. Miyata Y, Nishida E. CK2 Controls Multiple Protein Kinases by Phosphorylating a Kinase-Targeting Molecular Chaperone, Cdc37. *Molecular and Cellular Biology*. 2004; 24:4065–4074. [PubMed: 15082798]
37. Cozza G, Girardi C, Ranchio A, Lolli G, Sarno S, Orzeszko A, Kazimierczuk Z, Battistutta R, Ruzzene M, Pinna L. Cell-permeable dual inhibitors of protein kinases CK2 and PIM-1: structural features and pharmacological potential. *Cell. Mol. Life Sci*. 2014:1–13.

38. Cozza G, Mazzorana M, Papinutto E, Bain J, Elliott M, di Maira G, Gianoncelli A, Pagano MA, Sarno S, Ruzzene M, Battistutta R, Meggio F, Moro S, Zagotto G, Pinna LA. Quinalizarin as a potent, selective and cell-permeable inhibitor of protein kinase CK2. *The Biochemical journal*. 2009; 421:387–395. [PubMed: 19432557]
39. Battistutta R. Protein kinase CK2 in health and disease: Structural bases of protein kinase CK2 inhibition. *Cell Mol Life Sci*. 2009; 66:1868–1889. [PubMed: 19387547]
40. Cozza G, Bortolato A, Moro S. How druggable is protein kinase CK2? *Med Res Rev*. 2010; 30:419–462. [PubMed: 19526464]
41. Pagano MA, Bain J, Kazimierczuk Z, Sarno S, Ruzzene M, Di maira G, Elliott M, Orzeszko A, Cozza G, Meggio F, Pinna LA. The selectivity of inhibitors of protein kinase CK2: an update. *Biochemical Journal*. 2008; 415:353–365. [PubMed: 18588507]
42. Bish RA, Fregoso OI, Piccini A, Myers MP. Conjugation of complex polyubiquitin chains to WRNIP1. *Journal of proteome research*. 2008; 7:3481–3489. [PubMed: 18613717]
43. Kudo N, Wolff B, Sekimoto T, Schreiner EP, Yoneda Y, Yanagida M, Horinouchi S, Yoshida M. Leptomycin B inhibition of signal-mediated nuclear export by direct binding to CRM1. *Experimental cell research*. 1998; 242:540–547. [PubMed: 9683540]
44. Soderholm JF, Bird SL, Kalab P, Sampathkumar Y, Hasegawa K, Uehara-Bingen M, Weis K, Heald R. Importazole, a small molecule inhibitor of the transport receptor importin-beta. *ACS Chem Biol*. 2011; 6:700–708. [PubMed: 21469738]
45. Yata K, Lloyd J, Maslen S, Bleuyard JY, Skehel M, Smerdon SJ, Esashi F. Plk1 and CK2 act in concert to regulate Rad51 during DNA double strand break repair. *Molecular cell*. 2012; 45:371–383. [PubMed: 22325354]
46. Guerra B, Iwabuchi K, Issinger OG. Protein kinase CK2 is required for the recruitment of 53BP1 to sites of DNA double-strand break induced by radiomimetic drugs. *Cancer Letters*. 2014; 345:115–123. [PubMed: 24333722]
47. Durocher Y, Perret S, Kamen A. High-level and high-throughput recombinant protein production by transient transfection of suspension-growing human 293-EBNA1 cells. *Nucleic Acids Res*. 2002; 30:E9. [PubMed: 11788735]
48. Bradford MM. A rapid and sensitive method for the quantitation of microgram quantities of protein utilizing the principle of protein-dye binding. *Anal Biochem*. 1976; 72:248–254. [PubMed: 942051]
49. Al-Salihi MA, Herhaus L, Macartney T, Sapkota GP. USP11 augments TGF $\beta$  signalling by deubiquitylating ALK5. *Open Biology*. 2012; 2
50. Vogt J, Dingwell KS, Herhaus L, Gourlay R, Macartney T, Campbell D, Smith JC, Sapkota GP. Protein associated with SMAD1 (PAWS1/FAM83G) is a substrate for type I bone morphogenetic protein receptors and modulates bone morphogenetic protein signalling. *Open Biology*. 2014; 4
51. Campbell D, Morrice N. Identification of protein phosphorylation sites by a combination of mass spectrometry and solid phase Edman sequencing. *Journal of Biomolecular Techniques*. 2002; 13:119–130. [PubMed: 19498976]
52. Herhaus L, Al-Salihi M, Dingwell KS, Cummins TD, Wasmus L, Vogt J, Ewan R, Bruce D, Macartney T, Weidlich S, Smith JC, Sapkota GP. USP15 targets ALK3/BMPRI1A for deubiquitylation to enhance bone morphogenetic protein signalling. *Open Biology*. 2014; 4:140065. [PubMed: 24850914]

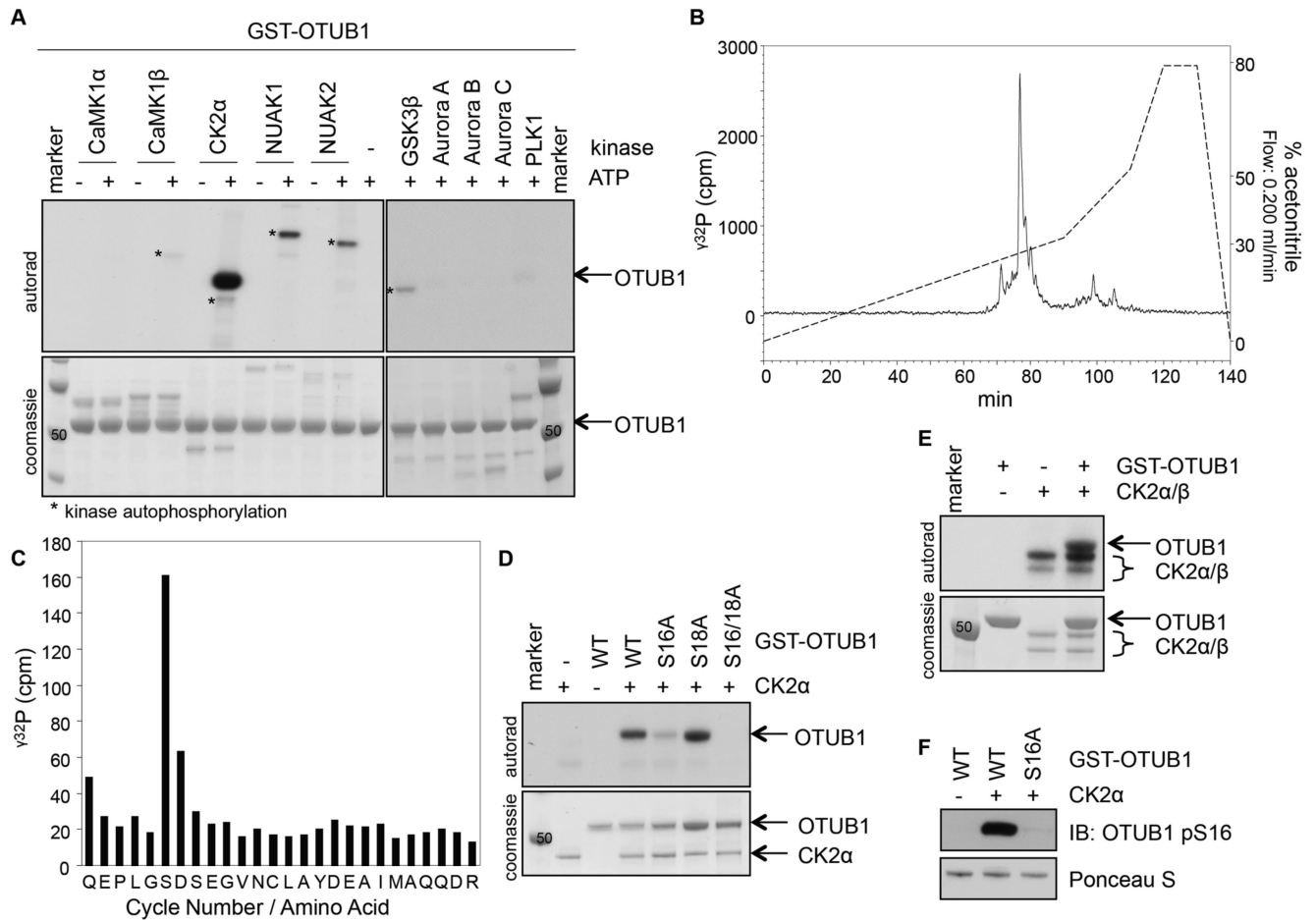


**Figure 1. OTUB1 is phosphorylated by CK2 in vitro**

(A) Coomassie stain and autoradiography of SDS-PAGE after an in vitro kinase assay with various kinases and GST-OTUB1 as the substrate. (B)  $\gamma^{32}\text{P}$ -release chromatogram of CK2-phosphorylated GST-OTUB1, which was digested with trypsin and resolved by HPLC on a C<sub>18</sub> column on an increasing acetonitrile gradient as shown. (C)  $\gamma^{32}\text{P}$  radioactivity release of the peak after each cycle of Edman degradation. (D) Coomassie stain and autoradiography of SDS-PAGE after an in vitro kinase assay with CK2 $\alpha$  and wild-type (WT) or various mutants of GST-OTUB1. (E) As in (D), with the holoenzyme CK2 $\alpha/\beta$  used as the kinase and GST-OTUB1 as the substrate. (F) Western blot (IB) of the phosphorylation of OTUB1 at Ser<sup>16</sup> (pS16) after the in vitro kinase assay as in (D). Total GST-OTUB1 was detected with Ponceau S. All blots are representative of 3 independent experiments.

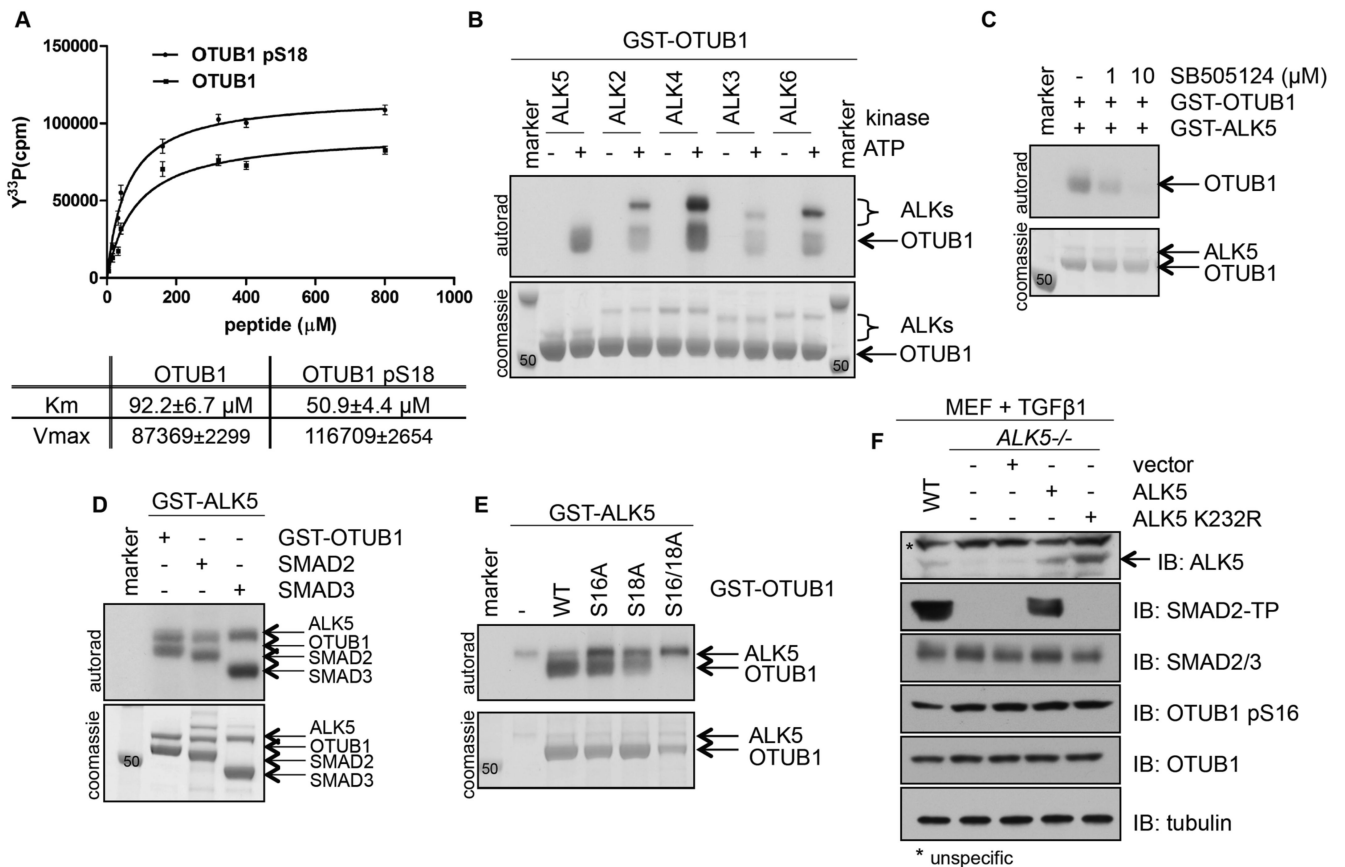


**Figure 2. ALKs can phosphorylate OTUB1, but phosphorylation of OTUB1 at Ser<sup>16</sup> is specific to CK2**

(A) Kinetics of an in vitro kinase assay assessing CK2 $\alpha$ -mediated phosphorylation of increasing amounts of OTUB1 and pSer<sup>18</sup>-OTUB1 peptides. The Km and Vmax values are indicated. Data are mean  $\pm$  S.D. from 3 experiments. (B) Coomassie stain and autoradiography of an in vitro kinase assay with different ALKs and GST-OTUB1. (C) As in (B), with GST-ALK5 and GST-OTUB1 in the presence of increasing amounts of the ALK5 inhibitor SB505124. (D) As in (B), with GST-ALK5 and SMAD2, SMAD3 and GST-OTUB1. (E) As in (B), with GST-ALK5 and wild-type or mutant GST-OTUB1. (F) Western blotting (IB) for the indicated proteins in lysates from MEF cells (wild-type, ALK5<sup>-/-</sup> and ALK5<sup>-/-</sup> transfected with wild-type or kinase-deficient mutant ALK5) treated with TGF $\beta$  (50 pM, 1 hour). (SMAD2-TP: SMAD2 tail phosphorylated at residues Ser<sup>465</sup> and Ser<sup>467</sup>). All blots are representative of 3 independent experiments.

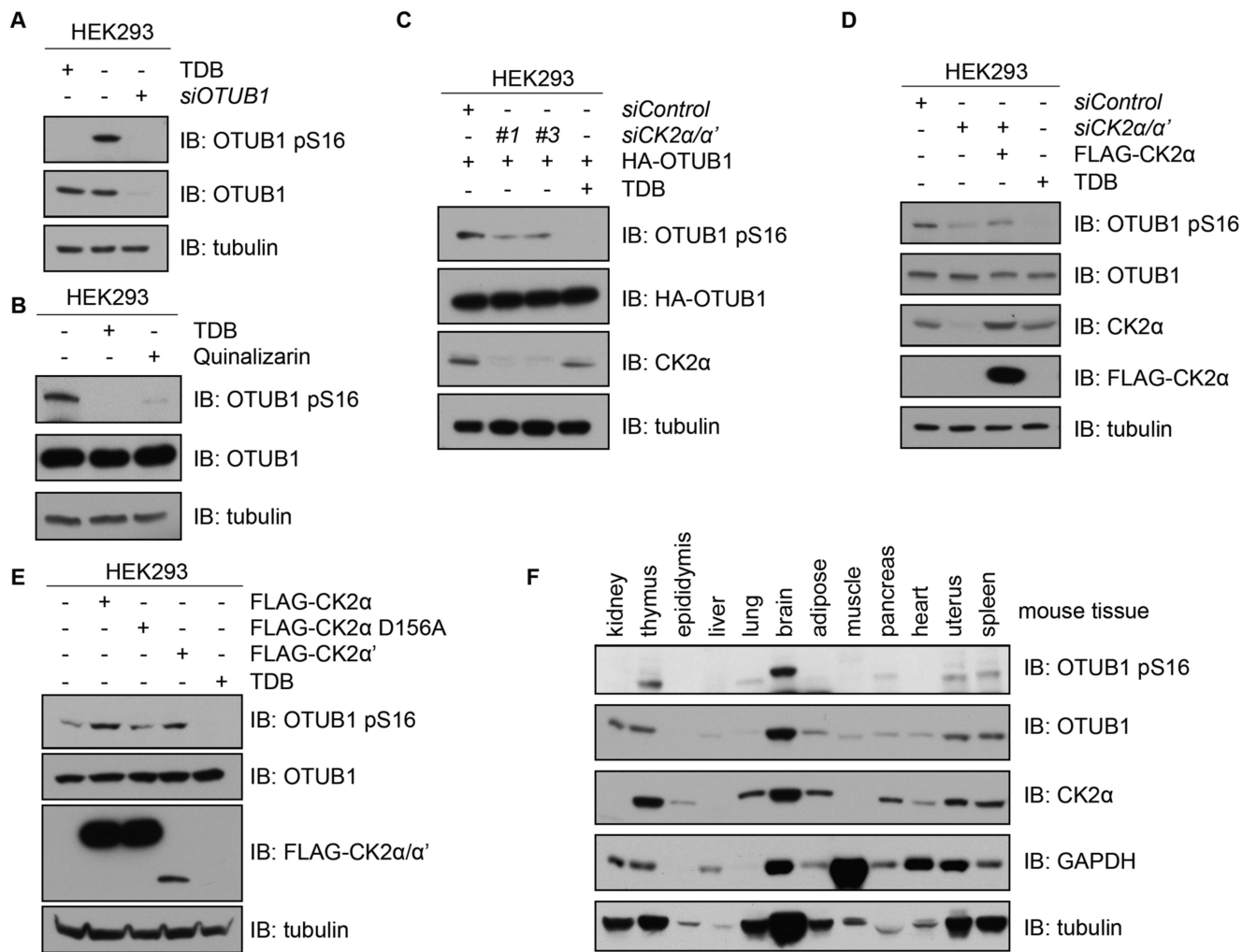


**Figure 3. CK2 phosphorylates OTUB1 in vivo**

(A) Western blotting (IB) of lysates from HEK293 cells that were untreated, treated with TDB (10  $\mu$ M, 4 hours) or transfected with *OTUB1* siRNA and lysed 48 hours later. (B) Western blotting (IB) of lysates from HEK293 cells that were untreated or, treated with TDB (10  $\mu$ M, 4 hours) or quinalizarin (10  $\mu$ M, 4 hours). (C) Western blotting (IB) of lysates from HEK293 cells transfected with HA-OTUB1 and *FOXO4* siRNA (siControl) or one of two siRNAs against both *CK2α* and *CK2α'* splice variants. A separate culture of cells was treated with TDB (10  $\mu$ M, 4 hours). (D) Western blotting (IB) of lysates from HEK293 cells transfected with *FOXO4* siRNA (control) or *CK2α/α'* siRNA alone or reconstituted with N-terminal FLAG-tagged CK2α. A separate culture of cells was treated with TDB (10  $\mu$ M, 4 hours) prior to lysis. (E) Western blotting (IB) of lysates from HEK293 cells transfected with vectors encoding N-terminal FLAG-tagged CK2α, FLAG-CK2α[D156A] or FLAG-CK2α', or treated with TDB (10  $\mu$ M, 4 hours). (F) Western blotting of homogenized lysates from the indicated mouse tissues. All blots are representative of 3 independent experiments.

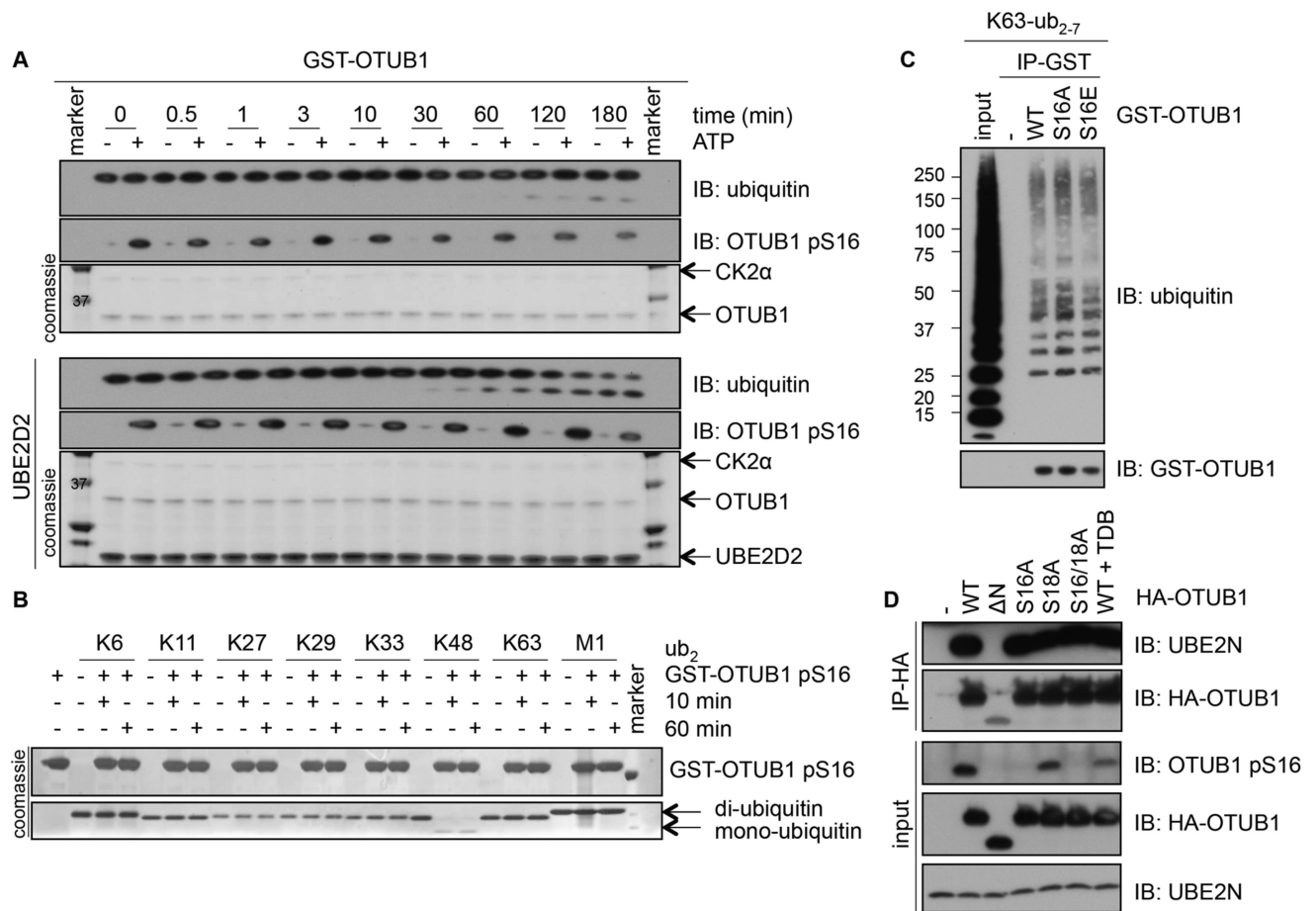


**Figure 4. The catalytic activity, ubiquitin- or E2-binding ability of OTUB1 are not altered by OTUB1 Ser<sup>16</sup> phosphorylation**

(A) A time course of K48-diubiquitin cleavage assay using unphosphorylated or in vitro CK2-phosphorylated OTUB1 (0.5  $\mu$ M), in the absence (top panel) or presence of UBE2D2 (bottom panel). Coomassie stains of OTUB1, CK2 $\alpha$  and UBE2D2 or Western blotting (IB) of ubiquitin and the phosphorylation of OTUB1 at Ser<sup>16</sup> (pS16) are indicated. (B) As in (A), with phosphorylated GST-OTUB1 (5  $\mu$ M) incubated with K6-, K11-, K27-, K29-, K33-, K48-, K63-, or M1-di-ubiquitin chains for 10 and 60 min in the absence of UBE2D2 and Coomassie stains indicated. (C) Western blotting (IB) of GST (-), GST-OTUB1 (WT), GST-OTUB1-S16A (S16A) or GST-OTUB1-S16E (S16E) incubated in vitro with K63-linked polyubiquitin chains in an interaction assay. (D) Western blotting (IB) of lysates or HA-immunoprecipitates from HEK293 cells transfected with HA-OTUB1 or HA-OTUB1 mutants treated with or without TDB (10  $\mu$ M, 4 h). All blots are representative of 3 independent experiments.

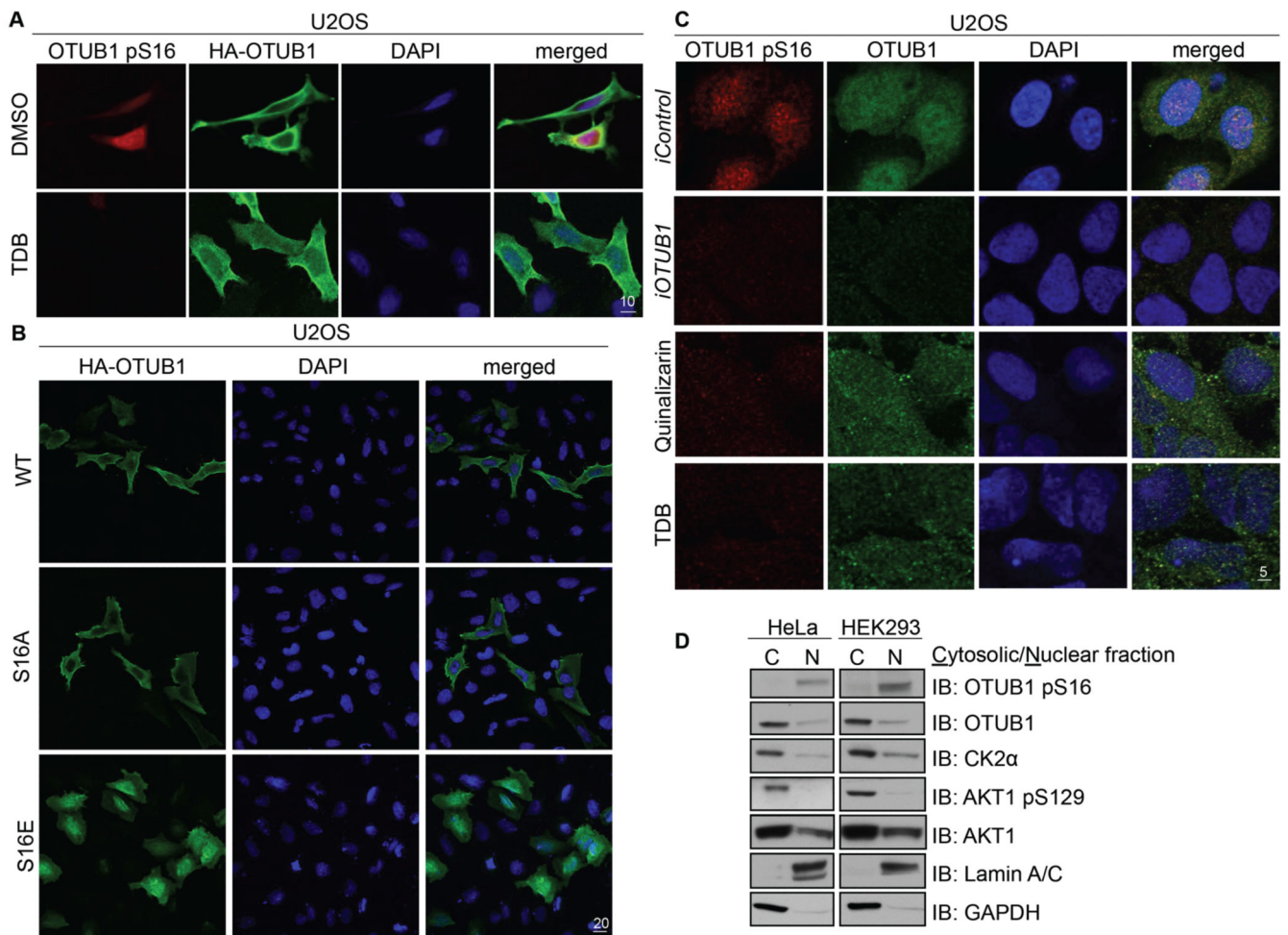


**Figure 5. OTUB1 phosphorylation at Ser<sup>16</sup> determines its subcellular localization**  
**(A)** Fixed cell immunofluorescence in U2OS cells transfected with HAOTUB1 and untreated or treated with TDB (10  $\mu$ M, 4 hours). Individual and merged images show phosphorylated OTUB1 pSer<sup>16</sup> (red), OTUB1 (HA, green) and DAPI (blue). Scale bar, 10  $\mu$ m. **(B)** As in (A) in U2OS cells transfected with HA-OTUB1, HA-OTUB1[S16A] or HA-OTUB1[S16E]. Scale bar, 20  $\mu$ m. **(C)** As in (A) in U2OS cells 48 hours after RNA interference [*iOTUB1* or *iControl* (*FOXO4*)] or after treatment with CK2 inhibitors quinalizarin (10  $\mu$ M, 4 hours) or TDB (10  $\mu$ M, 4 hours). Scale bar, 5  $\mu$ m. **(D)** Western blotting (IB) for the indicated proteins in cytosolic and nuclear fractions from HeLa or HEK293 cells. All data are representative of 3 independent experiments.

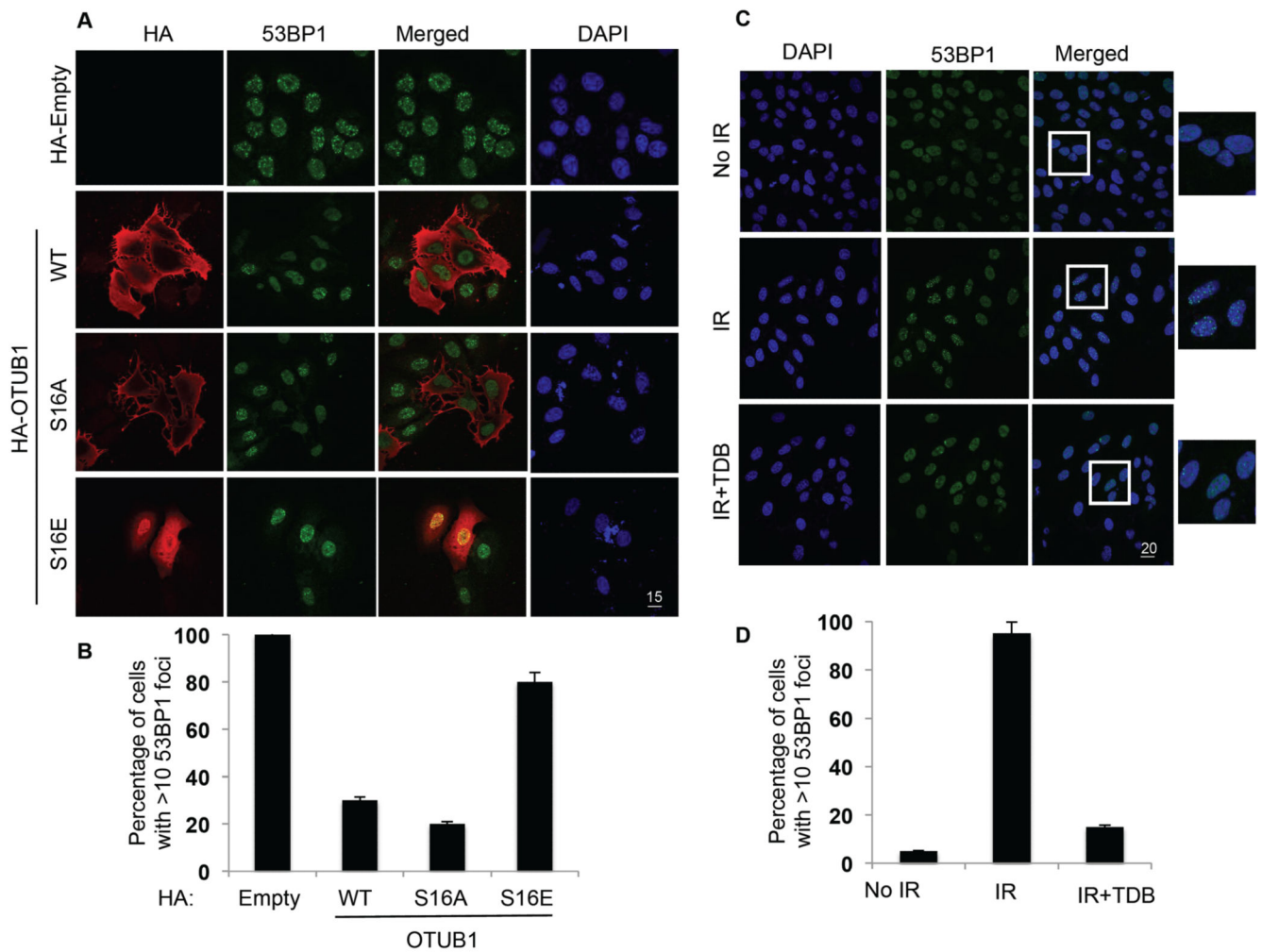


**Figure 6. The phosphorylation and nuclear localization of OTUB1 promotes IR-induced 53BP1 foci formation**

(A) Fixed cell immunofluorescence for OTUB1 localization and 53BP1 foci in U2OS cells transfected with HA-tag (HA-Empty), wild-type (WT) or mutant (S16E or S16A) HA-tagged OTUB1, then exposed to 5 Gy IR and fixed 3.5 hours later. Scale bar, 15  $\mu$ m. (B) Quantification of cells displaying more than 10 53BP1 foci from each condition in (A). (C) Fixed cell immunofluorescence in U2OS cells exposed to 5 Gy IR alone or treated with TDB (10  $\mu$ M, 4 hours) prior to IR exposure. Individual and merged pictures are shown displaying 53BP1 foci formation in green and DAPI in blue. Scale bar, 20  $\mu$ m. (D) Quantification as in (B). Images are representative, and data are mean  $\pm$  S.D. from 3 experiments, at least 33 cells quantified in each.